Statement. This is the first author version of the book chapter 10.1201/9780429022951-25 first published online by Taylor & Francis Group.

RADIATION (INDUCED) SYNTHESIS

Lorentz JÄNTSCHI[1], Sorana D. BOLBOACĂ[2]

[1] Technical University of Cluj-Napoca
[2] Iuliu Haţieganu University of Medicine and Pharmacy Cluj-Napoca

DEFINITION

Radiation (induced) synthesis refers conducting of a synthesis in the presence of a radiation of a certain type (of massless or of massive particles; of electrically charged or neutral particles) and with a certain wavelength or energy. In a Radi-synth process products are favoured against others by the use of the radiation. In this category fits Sound (induced) synthesis (or Sono(-)chemistry) which usually initiates or enhances the chemical activity in solutions, Ultrasound (assisted) synthesis (or ultrasonication) which have an extensive use in many industrial syntheses (including for solid phase products), Microwave synthesis which usually increases the temperature in the process, and Gamma-radiation (induced) synthesis with use in preparation of certain solid-state nanocompounds.

KEYWORDS:

Radiation chemistry; Sonochemistry; Sonication; Ultrasonication; Microwave synthesis; Gamma radiation induced synthesis

HISTORICAL ORIGIN(S)

In conventional chemical synthesis or chemosynthesis, the transformation of the reactive into the products can be facilitated by the use of the catalysts. In the presence of a catalyst, less free energy is required to reach the transition state, but the total free energy from reactants to products does not change (IUPAC 1997[1]). Catalyzed reactions have lower activation energy (rate-limiting free energy of activation) than the corresponding uncatalyzed reaction, resulting in a higher reaction rate at the same temperature and for the same reactant concentrations. Kinetically, catalytic reactions are typical chemical reactions; i.e. the reaction rate depends on the frequency of contact of the reactants in the rate-determining step. The SI derived unit for measuring the catalytic activity of a catalyst is the katal, which are moles per second. The productivity of a catalyst can be described by the turn over number (or TON) and the catalytic activity by the turn over frequency (TOF), which is the TON per time unit.

Catalysts work by providing an (alternative) mechanism involving different transition state and lower activation energy (see Figure 1 adapted from Jäntschi 2002[2]).

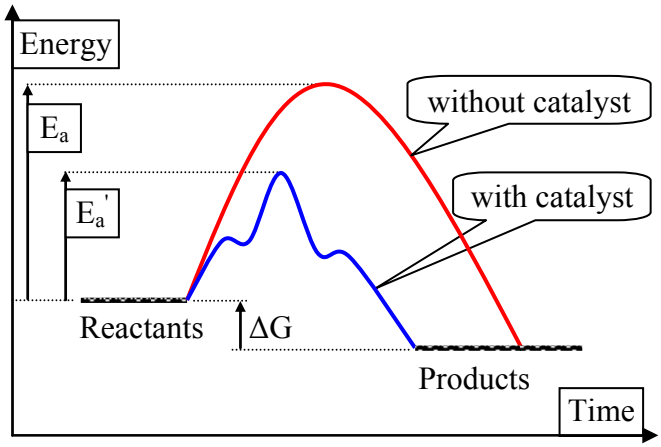

Figure 1. Generic influence of a catalyst to a chemical reaction

Radiation interacts with the matter at different levels when is charged or not and when contain massive particles or not. Different types of radiation serve the purpose of the Radi-Synth (see Table 1).

Table 1. Different types of radiations used in radiation (induced) synthesis

Radiation	Mass	Charge	Examples of uses
α (=He^{2+})	Yes (4 a.u.)	2+	(Haertling et al. 2011[3])
n	Yes (1 a.u.)	0	(Viererbl et al. 2014[4])
p (=H^{1+})	Yes (1.a.u.)	1+	(Crowell et al. 2005[5])
β (=e^-)	No	1-	(Oulianov et al. 2007[6])
EM	No	No	(Khan et al. 2006[7])

The most extensive work was conducted on the use of the electromagnetic (EM) radiation (γ, X, UV, VIS, IR, μW, Radio). The following table connects the wavelength of the radiation with its typical effects on the matter (see Table 2 translated and adapted from Jäntschi 2003[8]).

Table 2. Effects on the matter of electromagnetic radiations

Energy storage in matter	EM radiation		Wavelength (λ)	Radi-Synth refs
Molecular rotation	Radio		> 1 m	(Wardman 1987[9])
	Microwave (μW)		1 m 1 mm	(Dom et al. 2015[10])
Molecular vibration	Far infrared		10^{-3} m 10^{-5} m	(Delor et al. 2014[11])
	Near infrared		10^{-6} m = 1 μm 700 nm	
Electronic excitation (HOMO level)	Red	Visible	700-620 nm	(Kumar & Francisco 2015[12])
	Green		560-510 nm	(Wang et al. 2015[13])
	Violet		450-400 nm	(Kitamura et al. 2014[14])
	Ultraviolet (UV)		10^{-7} m	(Huang et al. 2008[15])
Excitation of the electronic core	UV of vacuum		10^{-8} m 10^{-9} m = 1 nm	(Simakov, 2008[16])
	X rays		10^{-10} m = 1 Å 10^{-11} m 10^{-12} m = 1 pm	(Kameneva et al. 2015[17])
Nucleus excitation	γ rays		10^{-12}-10^{-13} m	(Hareesh et al. 2016[18])
	cosmic rays		< 10^{-14} m	(Bassez 2015[19])

NANO-SCIENTIFIC DEVELOPMENT(S)

It should be noted that it is a inverse proportionality between the wavelength of the radiation and its energy ($E = h \cdot c/\lambda$, $h = 6.626070040(81) \cdot 10^{-34}$ J·s, $c = 299792458$ m·s^{-1}, E is the energy and λ is the wavelength of the radiation), and therefore with the decreasing of the wavelength it is increased its energy and vice-versa.

In 1839, Becquerel (Becquerel 1839[20]) discovered that electrical current flowed between a pair of electrodes if one electrode was illuminated with UV light, the phenomenon being later referred as the Becquerel effect (Prevenslik 2003[21]).

The interaction between high-energy radiation (γ-rays, X-rays, electrons, and ion beams) and matter produces a large number (~$4 \cdot 10^4$ electrons per MeV of energy deposited) of non-thermal secondary low-energy electrons (Kaplan & Miterev, 1987[22]). Due to the inelastic collisions of these low-energy electrons with molecules and atoms they become thermalized within approximately one picosecond (Mozumder & Hatano 2004[23]) and produce distinct energetic species such as free radicals that are the primary driving forces in a wide variety of radiation-induced reactions (Xu et al. 2014[24]).

High energy radiations (such as are γ-rays) shown a series of advantages for preparation of nanowires (Rana & Chauhan 2014[25]), colloidal metal nanoparticles (Henglein & Meisel 1998[26]), polymeric hydrogels (Burillo et al. 2012[27]), graphene (Shahriary & Athawale 2015[28]), functionalized nanofibers (Han et al. 2015[29]) and other nanostructures (Cui et al. 2014[30]; Su et al. 2014[31]).

The wet method for producing of metallic nanoclusters deposited on surfaces is based on the dissociation of the water molecules, succeeded by the dissociation of secondary alcohols (such as is isopropanol) or acids (such as is formic acid) also present in the prepared media (see Table 3, adapted from Belloni 2006[32]). Then the metal is deposited from its ions from solution alkalinized (to a pH = 11 with NH_4OH in Chettibi et al., 2006[33]).

Table 3. Metallic nanoclusters growth mechanism

Initiation	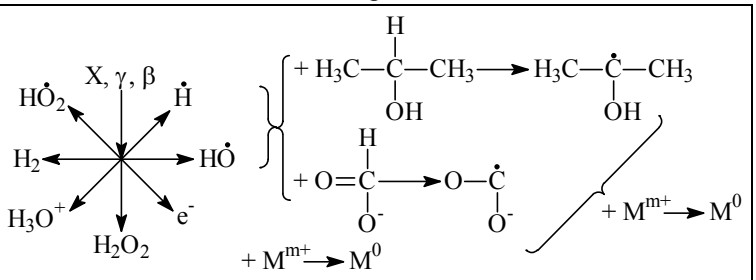
Propagation	$M_a + M^{m+} \rightarrow M_{a+1}^{m+}$, $a \geq 1$
Termination	$M_a^{m+} + e^- \rightarrow M_a$

Energetic excitation of a molecule may have follow routes to different intermediary products, as given below for electron-molecule interactions (Arumainayagam et al. 2010[34]):

÷ Electron impact ionization ($e^- + AB \rightarrow 2e^- + AB^{+*}$), having a short (relatively to the molecule passing time) interaction time (10^{-16} s), the incident electrons being necessary to have above 10 eV (ionization potential of a typical molecule) with a maximum yield at about 100 eV (Deutsch et al. 2000[35]). The ionized molecule may subsequently dissociate ($AB^{+*} \rightarrow A^+ + B^*$, or $AB^{+*} \rightarrow A^* + B^+$, or $AB^{+*} \rightarrow A^{+*} + B$ or $AB^{+*} \rightarrow A + B^{+*}$).

÷ Electron impact excitation ($e^- + AB \rightarrow e^- + AB^*$), when the incident electrons being necessary to have above 6 eV (excitation threshold for small organic molecules). A series of competing decay channels may be followed by the excited neutral molecule ($AB^* \rightarrow AB$ + energy (thermal or light); $AB^* \rightarrow A^* + B$; $AB^* \rightarrow A + B^*$; $AB^* \rightarrow A^+ + B^-$; $AB^* \rightarrow A^- + B^+$). Please note that the structures observed very infrequently at electron energies above the threshold for dipolar dissociation have usually been attributed to multiple electron-scattering prior to electron attachment (see Sambe et al. 1987[36]).

÷ Electron attachment ($e^- + AB \rightarrow AB^-$), producing a transient negative ion and occurring at low energies of the incident electrons (below 15 eV). The electron takes a position in a LUMO level and usually has an antibonding character. The incoming electron's energy must lie in restricted range defined by the Franck-Condon transition (Frank 1926[37]; Condon 1926[38]) to a discrete final state (AB^- or AB^{-*}) given that the molecular orbital associated with this state exists at a specific energy. Large cross sections associated with electron attachment may be attributed to the resonant character of the process. Resonant scattering is characterized by interaction times longer than the typical molecular transit times (which are typically less than 10^{-15} s) while the lifetime of a temporary negative ion ranges from 10^{-15} s to 10^{-2} s. Depending on whether the resonance is above or below the corresponding ground state (0-5 eV) or core-excited state (5-15 eV) of the neutral molecule, resonances may be further classified as either open channel (shape) or closed channel (Feshbach) resonances, respectively (Feshbach 1958[39]).

÷ Autodetachment ($AB^{-*} \rightarrow e^- + AB$ or $AB^{-*} \rightarrow e^- + AB^*$ as subsequent process of $e^- + AB \rightarrow AB^{-*}$). The autodetachment lifetimes vary from 10^{-14} s to 10^{-3} s (Illenberger 1992[40]), when as expected, complex molecules typically have long autodetachment lifetimes. Typically formed via resonances at near 0 eV, temporary negative ions for such molecules can often be detected by mass spectrometry because these ions do not undergo dissociation.

÷ Associative attachment and non-dissociative attachment ($AB^{-*} \rightarrow AB^-$ + energy), typical for clusters and condensed phase, when the energy is passed to neighbouring molecules (as thermal energy). Associative attachment (resonance stabilization) involves the attachment of an electron to a molecule via capture into a transient negative ion state lying above the vacuum level while non-dissociative attachment, leads to the production of a long-lived negative ion that can be detected with mass spectrometry. Such a mechanism were observed for molecules such as SF_6, C_6F_6, and C_{60} because their molecular complexity allows efficient intramolecular vibration redistribution (IVR) resulting in the formation of a metastable anion (Hotop et al. 2004[41]).

÷ Radiative cooling ($AB^{-*} \rightarrow AB^- + \gamma$). This channel is open only to molecules with a positive electron affinity and it involves relaxation via photon emission without being a significant competing one because radiative lifetimes are on the order of 10^{-8} s to 10^{-9} s (being much slower than the other ones).

It should be accounted that the branching ratio among the competing decay channels for the temporary negative ion is dependent on the state and phase (Illenberger 2003[42]). In addition, because of the large de Broglie wavelength (~12 Å for a 1 eV e^-) of low-energy incident electrons, the interaction of such electrons with the condensed phase must be treated theoretically as a multiple scattering problem (Ingolfsson et al. 1996[43]).

NANO-CHEMICAL APPLICATION(S)

Since the first report of microwave-assisted organic synthesis by the groups of Gedye (Gedye et al. 1986[44]) and Giguere (Giguere et al. 1986[45]), this technique become a tool for accelerating and controlling reactions, and increasing yields. Were introduced controlled, precise microwave reactors as an alternative to oil baths in an increasingly wide range of organic transformations (Mavandadi & Pilotti 2006[46]; Kappe & Dallinger 2006[47]).

The advantage of microwave technology in terms of heating can be applied to high-throughput techniques, such as solid-phase synthesis and polymer-assisted solution-phase synthesis. Synthesis of nano-sized structures may require the presence of a capping agent and/or of a support. Table 4 contains recently communicated results of Radi-synth using microwaves for different classes of nano-sized structures.

Table 4. Nano-sized structures recently developed with microwaves

Group	Structure	Capping agent	Support	Reference
metallic oxides	CeO_2	citric acid	-	He et al. 2016[48]
	CeO_2	ethylene glycol	TiO_2	Lu et al. 2016[49]
	CoO	-	-	Harish et al. 2016[50]
	Fe_2O_3	-	-	Sun et al. 2016[51]
	Fe_3O_4	-	polypyrrole	Yang et al. 2016[52]
	MoO_3	-	-	Wang et al. 2016[53]
	V_2O_5	oxalic acid	-	Pan et al. 2016[54]
	VO_x		SiO_2	Betiha et al. 2016[55]
double oxides	$BaFe_{12}O_{19}$	-	ethyl cellulose	Nabiyouni & Bakhtiari 2016[56]
	$ZnAl_2O_4$	-	-	Quirino et al. 2016[57]
salts	$LiFePO_4$	tetraethylene glycol	graphene oxide	Lim et al. 2016[58]
	$Mg_3(PO_4)_2$	-	-	Qi et al. 2016[59]
	Nd^{3+}-KY_3F_{10}	-	-	Orlovskii et al. 2016[60]
	CdS	polyvinylpyrrolidone	-	Darwish et al. 2016[61]
metals	Au, Ag	curdlan biopolymer	-	El-Naggar et al. 2016[62]
	Ag	l-Cysteine	-	Ma et al. 2016[63]
metallic mixes	Ru-Re	polyvinylpyrrolidone	Al_2O_3, SiO_2	Baranowska et al. 2016[64]
	Ti-Ni-Sn	-	-	Lei et al. 2016[65]
other	I_xB_{10}-I_yB_{12}	-	-	Juhasz et al. 2016[66]
	MWCNT	-	Ni	Bisht et al. 2016[67]

Sonic waves find their application in direct exfoliation and dispersion of two-dimensional materials (graphene, h-BN and MoS_2 were exfoliated in Kim et al. 2015[68]), sonochemical synthesis catalyzed by nanocomposites (polyhydroquinolines are obtained in Zarnegar et al. 2015[69]), obtaining of oxide nano-sized particles ($Cu_{0.88}Zn_{0.12}O$, Zn:CuO nano-sized particles were obtained in Eshedet al. 2014[70]) and acceleration of reactions (in general) in solution (reviewed in Fadeev et al. 2010[71]).

UV light (see Table 2) is often used for polymerization. In microfluidics, stop flow lithography (SFL) and optofluidic maskless lithography (OFML) can polymerize high-resolution 3D particles continuously by illuminating ultraviolet (UV) light on a static UV reactive fluid. Going further, Paulsen, et al. have developed a new optofluidic fabrication method that relies on two sequential steps: (1) highly controllable inertial flow shaping in microfluidic channels (Amini et al. 2013[72]) followed by (2) UV photopolymerization of the shaped fluid stream (Paulsen et al. 2015[73]). The optofluidic device uses two sheath fluid streams of polyethylene glycol diacrylate (PEG-DA) from the side channels,

sandwiching a photosensitive core fluid stream, PEG-DA with photoinitiator 2,2-dimethoxy-2-phenylacetophenone (DMPA).

High energy γ-rays (Lattach et al. 2013[74]; Lattach et al. 2014[75]; Cui et al. 2014[76]) as well as high energy electrons radiations (Coletta et al., 2015[77]) are used to generate oxidizing species, hydroxyl radicals, through water radiolysis, facilitating thus that subsequent activated monomers to polymerize. It was enabled the preparation of nanostructured PEDOT (PEDOTox) and PPy conducting polymers (Cui et al. 2016[78]).

MULTI-/TRANS- DISCIPLINARY CONNECTION(S)

Some studies have demonstrated that low-energy spin polarized secondary electrons, produced by X-ray irradiation of a magnetized Permalloy substrate, can induce chiral selective chemistry, which may explain the creation of 'handedness' in biological molecules, one of the great mysteries of the origin of life (Rosenberg et al., 2008[79]).

OPEN ISSUES

Ionising radiation exemplifies one of the conundrums of modern science because in the same time can be lethal and life-preserving. This dilemma extends to its applications such as the nuclear power and radiation sterilization of food products.

RELATED LIST OF ABBREVIATIONS

Radiolysis is the dissociation of molecules by nuclear radiation. It is the cleavage of one or several chemical bonds resulting from exposure to high-energy flux.

REFERENCES AND FURTHER READING

[1] IUPAC; 1997. "catalyst" in Compendium of Chemical Terminology, 2nd ed. Compiled by A. D. McNaught and A. Wilkinson. Oxford: Blackwell Scientific Publications.

[2] Jäntschi, L.; 2002. Chemical and instrumental analysis (in Romanian), Cluj-Napoca: UTPres.

[3] Haertling, C.; Usov, I.; Wang, Y.; 2011. Outgassing from alpha particle irradiation of lithium hydride and lithium hydroxide. Nuclear Instruments and Methods in Physics Research, Section B: Beam Interactions with Materials and Atoms 269(4): 444-451.

[4] Viererbl, L.; Klupák, V.; Vinš, M.; Lahodová, Z.; Kolmistr, A.; Stehno, J.; 2014. Radiation measurements after irradiation of silicon for neutron transmutation doping. Radiation Physics and Chemistry 95: 389-391.

[5] Crowell, R.A.; Shkrob, I.A.; Oulianov, D.A.; Korovyanko, O.; Gosztola, D.J.; Li, Y.; Rey-De-Castro, R.; 2005. Motivation and development of ultrafast laser-based accelerator techniques for chemical physics research. Nuclear Instruments and Methods in Physics Research, Section B: Beam Interactions with Materials and Atoms 241(1-4): 9-13.

[6] Oulianov, D.A.; Crowell, R.A.; Gosztola, D.J.; Shkrob, I.A.; Korovyanko, O.J.; Rey-De-Castro, R.C.; 2007. Ultrafast pulse radiolysis using a terawatt laser wakefield accelerator. Journal of Applied Physics 101(5): 053102.

[7] Khan, F.; Ahmad, S.R.; Kronfli, E.; 2006. γ-radiation induced changes in the physical and chemical properties of lignocellulose. Biomacromolecules 7(8): 2303-2309.

[8] Jäntschi, L.; 2003. Physical chemistry. Chemical and instrumental analysis (in Romanian), Cluj-Napoca: AcademicDirect.

[9] Wardman, P.; 1987. The mechanism of radiosensitization by electron-affinic compounds. Radiation Physics and Chemistry 30(5-6): 423-432.

[10] Dom, R.; Chary, A.S.; Subasri, R.; Hebalkar, N.Y.; Borse, P.H.; 2015. Solar hydrogen generation from spinel $ZnFe_2O_4$ photocatalyst: Effect of synthesis methods. International Journal of Energy Research 39(10): 1378-1390.

[11] Delor, M.; Scattergood, P.A.; Sazanovich, I.V.; Parker, A.W.; Greetham, G.M.; Meijer, A.J.H.M.; Towrie, M.; Weinstein, J.A.; 2014. Toward control of electron transfer in donor-acceptor molecules by bond-specific infrared excitation. Science 346(6216): 1492-1495.

[12] Kumar, M.; Francisco, J.S.; 2015. Red-Light-Induced Decomposition of an Organic Peroxy Radical: A New Source of the HO_2 Radical. Angewandte Chemie - International Edition DOI 10.1002/anie.201509311

[13] Wang, G.; Yuan, D.; Yuan, T.; Dong, J.; Feng, N.; Han, G.; 2015. A visible light responsive azobenzene-functionalized polymer: Synthesis, self-assembly, and photoresponsive properties. Journal of Polymer Science, Part A: Polymer Chemistry 53(23): 2768-2775.

[14] Kitamura, K.; Ieda, N.; Hishikawa, K.; Suzuki, T.; Miyata, N.; Fukuhara, K.; Nakagawa, H.; 2014. Visible light-induced nitric oxide release from a novel nitrobenzene derivative cross-conjugated with a coumarin fluorophore. Bioorganic and Medicinal Chemistry Letters 24(24): 5660-5662.

[15] Huang, L.; Zhai, M.L.; Long, D.W.; Peng, J.; Xu, L.; Wu, G.Z.; Li J.Q.; Wei G.S.; 2008. UV-induced synthesis, characterization and formation mechanism of silver nanoparticles in alkalic carboxymethylated chitosan solution. J Nanopart Res 10: 1193-1202.

[16] Simakov, M.B.; 2008. Asteroids and the origin of life - Two steps of chemical evolution on the surface of these objects. Earth, Planets and Space 60(1): 75-82.

[17] Kameneva, S.V.; Kobzarenko, A.V.; Feldman, V.I.; 2015. Kinetics and mechanism of the radiation-chemical synthesis of krypton hydrides in solid krypton matrices. Radiation Physics and Chemistry 110: 17-23.

[18] Hareesh, K.; Joshi, R.P.; Dahiwale, S.S.; Bhoraskar, V.N.; Dhole, S.D.; 2016. Synthesis of Ag-reduced graphene oxide nanocomposite by gamma radiation assisted method and its photocatalytic activity. Vacuum 124: 40-45.

[19] Bassez, M.-P.; 2015. Water, Air, Earth and Cosmic Radiation. Origins of Life and Evolution of Biospheres 45(1-2): 5-13.

[20] Becquerel, E.; 1839. Recherches sur les effets de la radiation chimique de la lumiere solaire au moyen des courants electriques. Comptes Rendus de L'Academie des Sciences 9: 145-149.

[21] Prevenslik, T.V.; 2003. The cavitation induced Becquerel effect and the hot spot theory of sonoluminescence. Ultrasonics 41(4): 313-317.

[22] Kaplan, I.G.; Miterev, A.M.; 1987. Interaction of Charged Particles with Molecular Medium and Track Effects in Radiation Chemistry. Advances in Chemical Physics 68: 255-386.

[23] Mozumder, A.; Hatano Y.; 2004. Charged Particle and Photon Interactions with Matter. New York: Marcel Dekker.

[24] Xu, H.; Fang, H.; Bai, J.; Zhang, Y.; Wang, Z.; 2014. Preparation and characterization of high-melt-strength polylactide with long-chain branched structure through γ-radiation-induced chemical reactions. Industrial and Engineering Chemistry Research 53(3): 1150-1159.

[25] Rana, P; Chauhan, R.P.; 2014. Size and irradiation effects on the structural and electrical properties of copper nanowires. Physica B: Condensed Matter 451: 26-33.

[26] Henglein, A.; Meisel D.; 1998. Radiolytic Control of the Size of Colloidal Gold Nanoparticles. Langmuir 14(26): 7392-7396.

[27] Burillo, G.; Castillo-Rojas, S.; Arrieta, H.; 2012. Cu(II) immobilization in AAc/NIPAAm-based polymer systems synthesized using ionizing radiation. Radiation Physics and Chemistry 81(3): 278-283.

[28] Shahriary, L.; Athawale, A.A.; 2015. Synthesis of graphene using gamma radiations. Bulletin of Materials Science 38(3): 739-745.

[29] Han, J.-M.; Wu, N.; Wang, B.; Wang, C.; Xu, M.; Yang, X.; Yang, H.; Zang, L.; 2015. γ radiation induced self-assembly of fluorescent molecules into nanofibers: A stimuli-responsive sensing. Journal of Materials Chemistry C 3(17): 4345-4351.

[30] Cui, Z.; Coletta, C.; Dazzi, A.; Lefrancois, P.; Gervais, M.; Néron, S.; Remita, S.; 2014. Radiolytic method as a novel approach for the synthesis of nanostructured conducting polypyrrole. Langmuir 30(46): 14086-14094.

[31] Su, F.; Miao, M.; Niu, H.; Wei, Z.; 2014. Gamma-irradiated carbon nanotube yarn as substrate for high-performance fiber supercapacitors. ACS Applied Materials and Interfaces 6(4): 2553-2560.

[32] Belloni J.; 2006. Nucleation, growth and properties of nanoclusters studied by radiation chemistry. Application to catalysis. Catalysis Today 113(3-4): 141-156.

[33] Chettibi, S.; Wojcieszak, R.; Boudjennad, E.H.; Belloni, J.; Bettahar, M.M.; Keghouche N.; 2006. Ni-Ce intermetallic phases in CeO_2-supported nickel catalysts synthesized by γ-radiolysis. Catalysis Today 113(3-4): 157-165.

[34] Arumainayagam, C.R.; Lee, H.-L.; Nelson, R.B.; Haines, D.R.; Gunawardane R.P.; 2010. Low-energy electron-induced reactions in condensed matter. Surface Science Reports 65: 1-44.

[35] Deutsch, H.; Becker, K.; Matt, S.; Mark, T.D.; 2000. Int. J. Mass Spectrom. 197(1): 37-69.

[36] Sambe, H.; Ramaker, D.E.; Parenteau, L.; Sanche, L.; 1987. Electron-stimulated desorption enhanced by coherent scattering. Phys. Rev. Lett. 59(4): 505-508.

[37] Franck, J.; 1926. Elementary processes of photochemical reactions. Transactions of the Faraday Society 21: 536-542.

[38] Condon, E.; 1926. A theory of intensity distribution in band systems. Physical Review 28: 1182-1201.

[39] Feshbach, H.; 1958. Unified theory of nuclear reactions. Annals of Physics 5(4): 357-390.

[40] Illenberger, E.; 1992. Electron-attachment reactions in molecular clusters. Chem. Rev. 92(7): 1589-1609.

[41] Hotop, H.; Ruf, M.W.; Allan, M.; Fabrikant, I.I.; 2004. Resonance threshold phenomena in low-energy electron collisions with molecules and clusters. Physica Scripta T110: 22-31.

[42] Illenberger, E.; 2003. Formation and evolution of negative ion resonances at surfaces. Surf. Sci. 528(1-3): 67-77.

[43] Ingolfsson, O.; Weik, F.; Illenberger, E.; 1996. The reactivity of slow electrons with molecules at different degrees of aggregation: gas phase, clusters and condensed phase. International Journal of Mass Spectrometry and Ion Processes 155(1): 1-68.

[44] Gedye, R.; Smith, F.; Westaway, K.; Ali, H.; Baldisera, L.; Laberge, L.; Rousell J.; 1986. The use of microwave ovens for rapid organic synthesis. Tetrahedron Lett. 27: 279-282.

[45] Giguere, R.J.; Bray T.L.; Duncan, S.M.; Majetich, G.; 1986. Application of commercial microwave ovens to organic synthesis. Tetrahedron Lett. 27: 4945-4948.

[46] Mavandadi, F.; Pilotti, A.; 2006. The impact of microwave-assisted organic synthesis in drug discovery. Drug Discov. Today 11(3-4): 165-174.

[47] Kappe, C.O.; Dallinger, D.; 2006. The impact of microwave synthesis on drug discovery. Nat. Rev. Drug Discov. 5: 51-63.

[48] He, D.; Hao, H.; Chen, D.; Lu, J.; Zhong, L.; Chen, R.; Liu, F.; Wan, G.; He, S.; Luo, Y.; 2016. Rapid synthesis of nano-scale CeO_2 by microwave-assisted sol-gel method and its

application for CH3SH catalytic decomposition. Journal of Environmental Chemical Engineering 4(1): 311-318.

[49] Lu, X.; Li, X.; Qian, J.; Miao, N.; Yao, C.; Chen, Z.; 2016. Synthesis and characterization of CeO2/TiO2 nanotube arrays and enhanced photocatalytic oxidative desulfurization performance. Journal of Alloys and Compounds 661: 363-371.

[50] Harish, S.; Silambarasan, K.; Kalaiyarasan, G.; Narendra Kumar, A.V.; Joseph, J.; 2016. Nanostructured porous cobalt oxide synthesis from $Co_3[Co(CN)_6]_2$ and its possible applications in Lithium battery. Materials Letters 165: 115-118.

[51] Sun, T.-W.; Zhu, Y.-J.; Qi, C.; Ding, G.-J.; Chen, F.; Wu, J.; 2016. α-Fe_2O_3 nanosheet-assembled hierarchical hollow mesoporous microspheres: Microwave-assisted solvothermal synthesis and application in photocatalysis. Journal of Colloid and Interface Science 463: 107-117.

[52] Yang, R.-B.; Reddy, P.M.; Chang, C.-J.; Chen, P.-A.; Chen, J.-K.; Chang, C.-C.; 2016. Synthesis and characterization of Fe_3O_4/polypyrrole/carbon nanotube composites with tunable microwave absorption properties: Role of carbon nanotube and polypyrrole content. Chemical Engineering Journal 285: 497-507.

[53] Wang, L.; Zhang, X.; Ma, Y.; Yang, M.; Qi, Y.; 2016. Rapid microwave-assisted hydrothermal synthesis of one-dimensional MoO3 nanobelts. Materials Letters 164: 623-626.

[54] Pan, J.; Li, M.; Luo, Y.; Wu, H.; Zhong, L.; Wang, Q.; Li, G.; 2016. Microwave-assisted hydrothermal synthesis of V_2O_5 nanorods assemblies with an improved Li-ion batteries performance. Materials Research Bulletin 74: 90-95.

[55] Betiha, M.A.; Rabie, A.M.; Elfadly, A.M.; Yehia, F.Z.; 2016. Microwave assisted synthesis of a VO_x-modified disordered mesoporous silica for ethylbenzene dehydrogenation in presence of CO_2. Microporous and Mesoporous Materials 222: 44-54.

[56] Nabiyouni, G.; Bakhtiari, M.; 2016. Microwave-assisted synthesis of BaFe12O19 nanoparticles and ethyl cellulose-based magnetic nanocomposite. Synthesis and Reactivity in Inorganic, Metal-Organic and Nano-Metal Chemistry 46: 163-167.

[57] Quirino, M.R.; Oliveira, M.J.C.; Keyson, D.; Lucena, G.L.; Oliveira, J.B.L.; Gama, L.; 2016. Synthesis of zinc aluminate with high surface area by microwave hydrothermal method applied in the transesterification of soybean oil (biodiesel). Materials Research Bulletin 74: 124-128.

[58] Lim, J.; Gim, J.; Song, J.; Nguyen, D.T.; Kim, S.; Jo, J.; Mathew, V.; Kim, J.; 2016. Direct formation of $LiFePO_4$/graphene composite via microwave-assisted polyol process. Journal of Power Sources 304: 354-359.

[59] Qi, C.; Zhu, Y.-J.; Wu, C.-T.; Sun, T.-W.; Chen, F.; Wu, J.; 2016. Magnesium phosphate pentahydrate nanosheets: Microwave-hydrothermal rapid synthesis using creatine phosphate as an organic phosphorus source and application in protein adsorption. Journal of Colloid and Interface Science 462: 297-306.

[60] Orlovskii, Y.V.; Vanetsev, A.S.; Keevend, K.; Kaldvee, K.; Samsonova, E.V.; Puust, L.; Del Rosal, B.; Jaque, D.; Ryabova, A.V.; Baranchikov, A.E.; Lange, S.; Sildos, I.; Kikas, J.; Loschenov, V.B.; 2016. NIR fluorescence quenching by OH acceptors in the Nd^{3+} doped KY_3F_{10} nanoparticles synthesized by microwave-hydrothermal treatment. Journal of Alloys and Compounds 661: 312-321.

[61] Darwish, M.; Mohammadi, A.; Assi, N.; 2016. Microwave-assisted polyol synthesis and characterization of pvp-capped cds nanoparticles for the photocatalytic degradation of tartrazine. Materials Research Bulletin 74: 387-396.

[62] El-Naggar, M.E.; Shaheen, T.I.; Fouda, M.M.G.; Hebeish, A.A.; 2016. Eco-friendly microwave-assisted green and rapid synthesis of well-stabilized gold and core-shell silver-gold nanoparticles. Carbohydrate Polymers 136: 1128-1136.

[63] Ma, Y.; Pang, Y.; Liu, F.; Xu, H.; Shen, X.; 2016. Microwave-assisted ultrafast synthesis of silver nanoparticles for detection of Hg^{2+}. Spectrochimica Acta - Part A: Molecular and Biomolecular Spectroscopy 153: 206-211.

[64] Baranowska, K.; Okal, J.; Tylus, W.; 2016. Microwave-assisted polyol synthesis of bimetallic RuRe nanoparticles stabilized by PVP or oxide supports (γ-alumina and silica). Applied Catalysis A: General 511: 117-130.

[65] Lei, Y.; Li, Y.; Xu, L.; Yang, J.; Wan, R.; Long, H.; 2016. Microwave synthesis and sintering of TiNiSn thermoelectric bulk. Journal of Alloys and Compounds 660: 166-170.

[66] Juhasz, M.A.; Matheson, G.R.; Chang, P.S.; Rosenbaum, A.; Juers, D.H.; 2016. Microwave-Assisted Iodination: Synthesis of Heavily Iodinated 10-Vertex and 12-Vertex Boron Clusters. Synthesis and Reactivity in Inorganic, Metal-Organic and Nano-Metal Chemistry 46(4): 583-588.

[67] Bisht, A.; Chockalingam, S.; Panwar, O.S.; Kesarwani, A.K.; Singh, B.P.; Singh, V.N.; 2016. Substrate bias induced synthesis of flowered-like bunched carbon nanotube directly on bulk nickel. Materials Research Bulletin 74: 156-163.

[68] Kim J.; Kwon S.; Cho D.-H.; Kang B.; Kwon H.; Kim Y.; Park S.O.; Jung G.Y.; Shin E.; Kim W.-G.; Lee H.; Ryu G.H.; Choi M.; Kim T.H.; Oh J.; Park S.; Kwak S.K.; Yoon S.W.; Byun D.; Lee Z.; Lee C.; 2015. Direct exfoliation and dispersion of two-dimensional materials in pure water via temperature control. Nature Communications 6: 8294.

[69] Zarnegar, Z.; Safari, J.; Kafroudi, Z.M.; 2015. Co_3O_4-CNT nanocomposites: A powerful, reusable, and stable catalyst for sonochemical synthesis of polyhydroquinolines. New Journal of Chemistry 39(2): 1445-1451.

[70] Eshed, M.; Lellouche, J.; Gedanken, A.; Banin, E.; 2014. A Zn-doped CuO nanocomposite shows enhanced antibiofilm and antibacterial activities against Streptococcus mutans compared to nanosized CuO. Advanced Functional Materials 24(10): 1382-1390.

[71] Fadeev, G.N.; Kuznetsov, N.N.; Beloborodova, E.F.; Matakova, S.A.; 2010. The influence of the acoustic resonance frequency on chemical reactions in solution. Russian Journal of Physical Chemistry A 84(13): 2254-2258.

[72] Amini, H.; Sollier, E.; Masaeli, M.; Xie, Y.; Ganapathysubramanian, B.; Stone H.A.; Di Carlo, D.; 2013. Engineering fluid flow using sequenced microstructures. Nat. Commun. 4: 1826.

[73] Paulsen, K.S.; Di Carlo, D.; Chung, A.J.; 2015. Optofluidic fabrication for 3D-shaped particles. Nat. Commun. 6: 6976.

[74] Lattach, Y.; Deniset-Besseau, A.; Guigner, J.M.; Remita, S.; 2013. Radiation chemistry as an alternative way for the synthesis of PEDOT conducting polymers under "soft" conditions. Radiat. Phys. Chem., 82: 44-53.

[75] Lattach, Y.; Coletta, C.; Ghosh, S.; Remita, S.; 2014. Radiation-induced synthesis of nanostructured conjugated polymers in aqueous solution: fundamental effect of oxidizing species. Chemphyschem 15: 208-218.

[76] Cui, Z.; Coletta, C.; Dazzi, A.; Lefrancois, P.; Gervais, M.; Neron, S.; Remita, S.; 2014. Radiolytic method as a novel approach for the synthesis of nanostructured conducting polypyrrole. Langmuir 30: 14086-14094.

[77] Coletta, C.; Cui, Z.; Archirel, P.; Pernot, P.; Marignier, J.L.; Remita, S.; 2015. Electron-induced growth mechanism of conducting polymers: a coupled experimental and computational investigation. J. Phys. Chem. B 119: 5282-5298.

[78] Cui, Z.; Coletta, C.; Rebois, R.; Baiz, S.; Gervais, M.; Goubard, F.; Aubert, P.-H.; Dazzi, A.; Remita, S.; 2016. Radiation Physics and Chemistry 119: 157-166.

[79] Rosenberg, R.A.; Abu Haija, M.; Ryan, P.J.; 2008. Phys. Rev. Lett. 101: 178301.